Journal of Environmental Ecology

https://jee.cultechpub.com/jee

E-ISSN: 3093-8074

Vol. 2, No. 2, October 2026

DOI: 10.64229/zedswe65

Article

Drivers, Spatial Extent, and Predicted Future Risk of Woody Vegetation Dynamics and Fragmentation in Kyle Recreational Park, Southern Zimbabwe

Enock Tapedzwa*, Fabian Bhasikiti

Centre for Wildlife Conservation and Research, Gwanda State University, Epoch Mine Campus, P.O. Box 30, Filabusi, Zimbabwe

*Corresponding author: Enock Tapedzwa, Enock.tapedzwa@gsu.ac.zw; etapedzwa@gmail.com

Abstract

Woody vegetation dynamics and fragmentation shape the ecological integrity of protected areas across southern Africa. This study combined remote sensing (RS), geographic information systems (GIS), and a structured questionnaire survey to identify the drivers, spatial extent, and future risk of woody vegetation change in Kyle Recreational Park, southern Zimbabwe, between 2016 and 2025. Dry- and wet-season Landsat 8 and 9 composites processed in Google Earth Engine (GEE) were classified with a Random Forest classifier into woodland, non-woody, and open-water classes within the 17,072 ha park boundary (overall accuracy 94.3% and 74.6%; Kappa 0.91 and 0.62 for 2016 and 2025, respectively). Gross and net change were separated with a transition matrix, fragmentation was quantified with class-level landscape metrics, and a questionnaire (n = 50) captured park-staff and community perceptions of drivers. Woodland increased from 4,724 ha to 6,051 ha (+28.1%), but this net gain combined 2,161 ha of gain with 834 ha of loss, so that 17.7% of the 2016 woodland was lost. Woodland patches became fewer and larger (number of patches −57%; mean patch size 4.2 to 12.6 ha; edge density −9%), indicating consolidation of the woodland matrix rather than landscape-wide fragmentation. Loss was concentrated at the margins: 25.3% of woodland at patch edges was lost, against 10.3% of woodland more than 120 m from an edge, and the loss rate within 1 km of the park boundary (21.6%) was 1.6 times that further inside (13.8%). A logistic model built on these gradients, with modest discrimination (spatially cross-validated AUC = 0.62), placed 1,755 ha (29%) of the 2025 woodland in a high-risk zone for future loss. The annual area of persistent decline in the Normalized Difference Vegetation Index (NDVI) increased by 115.9 ha yr^{-1} over 2018–2025 ($R^2 = 0.63$; $F(1, 6) = 10.02$; $p = 0.019$), partly coinciding with the 2023–2024 El Niño drought. Just over half of respondents (52%) identified anthropogenic pressures, chiefly agricultural encroachment, fire, illegal mining, and logging, as the principal drivers, with climate variability a secondary driver. Net woody expansion, consistent with bush encroachment and post-drought recovery, is therefore occurring alongside persistent, edge-concentrated loss. We recommend community-led co-management that reduces household dependence on park resources, targeted protection of the high-risk boundary zone, active management of bush encroachment, and routine monitoring, supported by enforcement of existing legislation.

Keywords

Landscape fragmentation, Bush encroachment, Edge effects, Land-use/land-cover change, Google Earth Engine, Risk mapping

Article History

Received: 28 July 2026
Revised: 16 November 2026
Accepted: 17 November 2026
Available Online: 27 November 2026

Copyright

© 2026 by the authors. This article is published by the Cultech Publishing Sdn. Bhd. under the terms of the Creative Commons Attribution 4.0 International License (CC BY 4.0): https://creativecommons.org/licenses/by/4.0

1. Introduction

Forest loss and fragmentation are among the most pressing challenges facing wildlife and protected-area management worldwide, with cumulative and often self-reinforcing effects on biodiversity. Both natural and anthropogenic factors drive changes in woody vegetation: climate change and human disturbance are widely regarded as the two dominant underlying forces [1,2]. Because vegetation loss and fragmentation reduce habitat area, connectivity, and quality, they are recognized as leading global drivers of biodiversity decline [3]. While the problem is global, it is most visible in developing and emerging economies, where economic development and population growth frequently outpace conservation capacity.

At the global scale, forest fragmentation results from processes operating across a wide range of spatial and temporal scales [4]. Geological and climatic forces reshape landscapes over long time frames, while natural disturbances (fire, flooding, landslides, and storms) can fragment vegetation abruptly. Some ecosystems are naturally patchy, and many species depend on this heterogeneity. Nonetheless, warming and prolonged drought are the climate-related pressures most consistently linked to woody-vegetation degradation [1], and the Intergovernmental Panel on Climate Change (IPCC) Sixth Assessment Report projects increasing aridity, more frequent drought and heat extremes, and heightened risks of biodiversity loss and ecosystem degradation across Africa this century [5]. Changing temperature and rainfall patterns are also associated with more frequent floods and droughts, shifting species ranges, densities, and growth rates [5,6].

Fire is a particularly important driver of vegetation structure across African savannas, shaping species composition and distribution except where fuel loads or moisture are insufficient to sustain a burn [7]. The frequency and intensity of fire is central to maintaining or eroding woody cover in savanna systems [7], and Africa is the continent most affected by fire: most global fire carbon emissions come from grassland and savanna burning [8], about half of global gas and particle emissions from fire originate in sub-Saharan Africa [9], and fire regimes are highly uneven across the continent's climatic zones [10].

In Zimbabwe, human activity is widely regarded as the leading cause of biodiversity loss. Deforestation, land degradation, uncontrolled fire, mining, road construction, land-use conflict, and invasive species are all implicated [11], compounded by an increased frequency of severe droughts and floods [12]. Agricultural expansion and mining are consistently identified as the leading proximate causes [13], and slash-and-burn cultivation has become an especially significant driver of forest loss [14]: an estimated 70,000 hectares of Zimbabwean woodland are cleared for agriculture each year [15]. Mining within protected areas carries particular risk, threatening both wildlife habitat and the tourism economies that depend on it [16]. Critically, these proximate pressures are underpinned by household economic dependence on woodland resources: for many households bordering protected areas, fuelwood, construction timber, grazing, arable land, and artisanal mining constitute primary or supplementary livelihood sources. Edge-boundary woodland exploitation is therefore best understood as the spatial expression of household-level economic need, concentrated where community lands meet the park boundary, rather than as isolated illegal behavior [12,15].

Despite ongoing efforts to conserve vegetation and wildlife habitat, woody-vegetation loss and fragmentation remain a persistent management challenge in Kyle Recreational Park. This study set out to identify the key drivers of woody-vegetation change and to map its spatial extent between 2016 and 2025, and to identify where the remaining woodland is at greatest risk of future loss. The study tested the null hypothesis that there was no significant temporal trend in the annual area of persistent vegetation decline, an index derived from the NDVI, between 2016 and 2025, against the alternative that a significant trend occurred. The annual NDVI series was chosen as the inferential test because the two-date classification yields only a single estimate of change in woodland area and in each fragmentation metric, which cannot be tested for a temporal trend, whereas the annual series provides repeated observations through time. Change in woodland fragmentation was quantified with discrete class-level metrics, namely the number of woodland patches (NP), mean patch size (MPS), edge density (ED), largest patch index (LPI), and core area; because each metric is a single summary of one map, its change between 2016 and 2025 is evaluated by direction and magnitude rather than by an inferential test.

2. Materials and Methods

2.1 Study Area

Kyle Recreational Park lies in south-eastern Zimbabwe, within Masvingo District, about 24 km south-east of Masvingo town (straight-line distance to the park centroid), centered near 20.1967°S, 30.9994°E [17] (Figure 1). The park was established following completion of the Kyle Dam in 1960, on land previously held communally by the Basutu and Kalanga peoples [18]. Published descriptions give an area of approximately 16,900 ha, of which the lake occupies roughly 9,300 ha when full and the terrestrial park approximately 7,600 ha, concentrated on the lake's northern shore with a smaller recreational area to the south. The digital boundary used in this study encloses 17,071.8 ha (planar area in the Universal Transverse Mercator [UTM] projection, zone 36S), and all area statistics reported here refer to this boundary (Figure 1c).

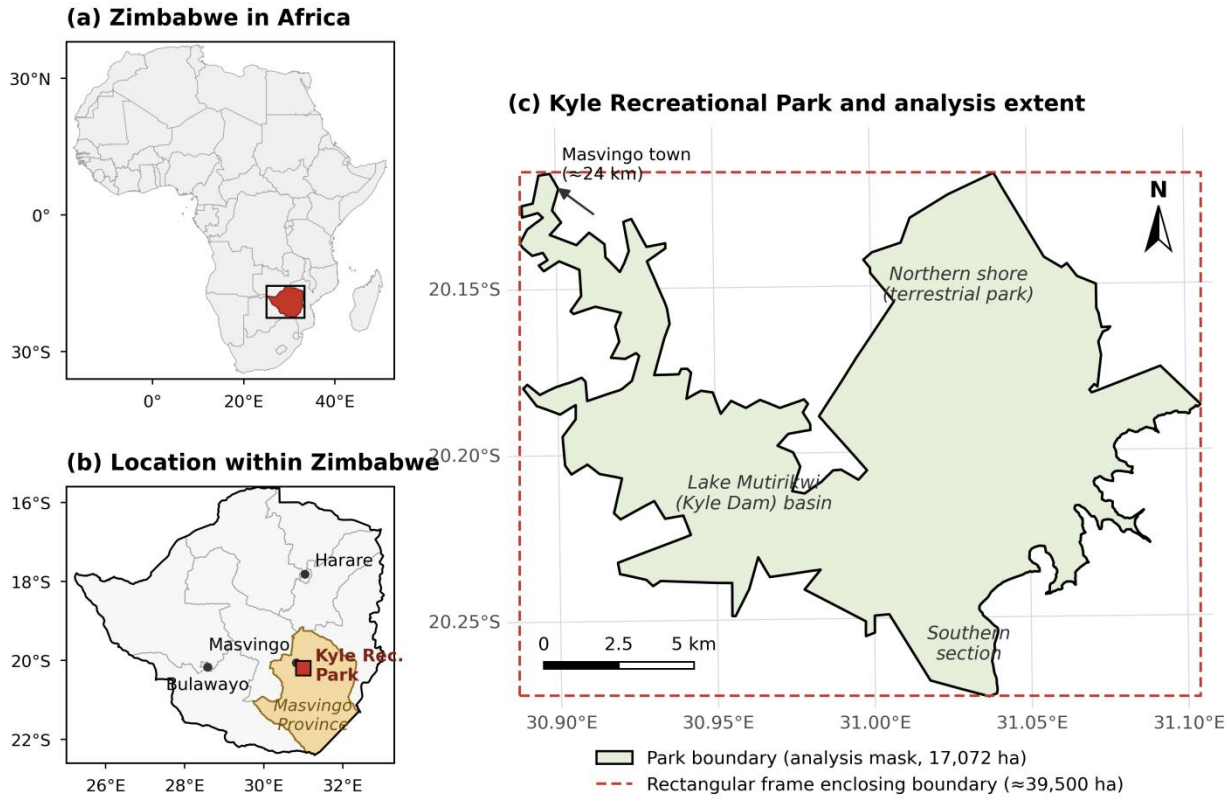

Figure 1. Location of Kyle Recreational Park: (a) Zimbabwe within Africa; (b) the park within Masvingo Province; (c) the park boundary used as the analysis mask (17,072 ha), showing the northern shore, the Lake Mutirikwi (Kyle Dam) basin, and the southern section, with the rectangular frame enclosing the boundary (≈39,500 ha), which approximates the 39,410 ha extent used in the original analysis. All statistics in this study are masked to the park boundary. Boundaries: Natural Earth [19]; projection of (c): WGS 84 / UTM zone 36S.

The park is bordered to the north by the Beza mountain range (rising to 1,485 m), with an undulating plain averaging 1,070 m between the mountains and the lake; elevation across the park ranges from 700 to 1,485 m, and broken hills divide the lake into eastern and western basins. The south is dominated by granite hills and exposed rock. Soils are spatially variable (fertile but capping-prone red clays derived from banded ironstone and schist in central areas, and less fertile sandy soils along the western boundary) and are uniformly deficient in phosphorus. Vegetation is predominantly mixed woodland and shrubland (Combretum, Acacia, Terminalia sericea), grading into riverine forest, open woodland, grassland, and rocky hill vegetation, with Miombo woodland transitioning into Peltophorum africanum–Acacia karoo thicket. The climate is subtropical savanna with a single rainy season (November–March) and mean annual rainfall of approximately 622 mm. Tourism, fishing, and wildlife-based recreation are the park's principal economic activities.

2.2 Remote Sensing Data and Classification

The study combined RS and GIS analysis with a questionnaire survey. Satellite data were processed in GEE, a cloud-based platform for planetary-scale geospatial analysis [20,21]. Landsat 8 Operational Land Imager (OLI) and Landsat 9 OLI-2 Collection 2 Level-2 surface-reflectance scenes were used to build, for each target year (2016 and 2025), a dry-season median composite (1 May–30 September; 10 scenes in 2016 and 19 in 2025) and a wet-season median composite (1 November of the preceding year to 31 March; 9 and 16 scenes, respectively). Clouds and cloud shadows were removed at the pixel level with the QA_PIXEL quality band, and each composite was clipped to the park boundary, so that the classification and all area statistics refer to the 17,072 ha park rather than to the rectangular frame enclosing it (Figure 1c). The classification used 11 predictors: dry-season blue, red, near-infrared, and two shortwave-infrared reflectance bands; dry-season NDVI, Normalized Difference Water Index (NDWI) [22], and Normalized Burn Ratio (NBR); the wet-minus-dry-season differences in NDVI and in the Soil-Adjusted Vegetation Index (SAVI) [23], which capture the seasonal senescence of the herbaceous layer relative to the more persistent woody canopy; and slope derived from the Shuttle Radar Topography Mission (SRTM) digital elevation model [24]. Images were classified with a Random Forest classifier of 100 trees [25], chosen for its accuracy and efficiency with high-dimensional geospatial data.

Reference points were digitized for five cover types (woodland, cropland, grassland, open water, and rock outcrop) by visual interpretation of false-colour (near-infrared–red–blue) composites, and separate reference sets were compiled for 2016 and 2025 so that each date was labelled against its own imagery. Preliminary five-class classifications did not reach acceptable accuracy (Kappa ≤ 0.54), with the lowest class accuracies for cropland, grassland, and rock outcrop, which form fine-grained, spectrally overlapping mosaics at the 30 m Landsat resolution. These three types were therefore merged

into a single non-woody class, and the final classification used three classes: woodland; non-woody (herbaceous cover, cultivated land, and bare and rock surfaces, including exposed lakebed); and open water. This aggregation retains the class of primary interest while avoiding the reporting of distinctions that the imagery could not support. For each date, reference points were randomly divided into 70% for training and 30% for validation before the classifier was trained, so that validation points played no part in model fitting.

No ground-control points were collected in the field. Training and validation labels were therefore assigned by visual interpretation of the dry-season false-colour composites and the seasonal NDVI difference layer, as described above, and the floristic composition of the mapped woodland could not be verified on the ground. The woodland class should accordingly be understood as woody canopy cover detectable at 30 m resolution: it includes mature woodland and riverine forest but can also include dense shrub thicket and encroaching woody regrowth, which are spectrally similar to closed woodland in Landsat imagery. Dry-season NDVI, computed for each image date, served as the baseline indicator of vegetation condition, and the wet-minus-dry-season NDVI difference supported separation of persistent woody canopy from seasonally senescent herbaceous cover.

Land-cover change was assessed by post-classification comparison of the 2016 and 2025 maps. Class areas were obtained by counting 30 m pixels (0.09 ha) inside the park boundary, and a cross-tabulation (transition matrix) of the two dates was computed for pixels with valid observations on both dates. Because net class change conceals offsetting gains and losses, gross gain, gross loss, net change, and swap change (twice the smaller of gain and loss, i.e. the change that cancels out in the net figure) were derived for each class [26]. A map of stable woodland, woodland gain, and woodland loss was produced from the same cross-tabulation.

2.3 Accuracy Assessment

Classification accuracy was assessed using overall accuracy and the Kappa coefficient, which accounts for chance agreement [27]. Because reliance on Kappa alone is increasingly discouraged in RS accuracy assessment [28], producer's and user's accuracies were also computed for each class from the confusion matrix, together with quantity and allocation disagreement [28]. Accuracy was evaluated on the withheld validation points ($n = 53$ for 2016 and $n = 67$ for 2025). Because the reference points were placed by image interpretation rather than by probability sampling, area-adjusted accuracy estimates and confidence intervals for class areas [29] could not be computed, and mapped areas are reported without error adjustment.

2.4 Fragmentation Metrics

Landscape fragmentation was quantified from the classified 2016 and 2025 maps using standard class-level landscape metrics for the woodland class: class area (CA), NP, patch density (PD), MPS, ED, LPI, and total core area (TCA). Metrics were computed in R with the landscapemetrics package [30], which implements the FRAGSTATS definitions [31], using the eight-neighbour patch rule and an edge depth of one cell (30 m) for core area. To prevent differences in reservoir level between the two dates from registering as woodland fragmentation, metrics were computed on the terrestrial landscape of each date, with open water set to no-data.

2.5 Questionnaire Survey

Questionnaires are a well-established tool for data collection in biodiversity conservation and policy research [32], comprising a standardized set of items designed to elicit data on a defined topic [33]. A structured questionnaire was administered to Kyle Recreational Park staff ($n = 30$) and to members of the surrounding community ($n = 20$) to capture perceptions of the drivers, extent, and management of woody-vegetation loss and fragmentation. Park staff were selected purposively to cover all occupational groups (rangers, ecologists, area managers, administrative and support staff, and general laborers), while community respondents were drawn from households in wards adjacent to the park boundary. The instrument comprised closed-ended items covering (i) socio-demographic characteristics; (ii) perceived drivers of woody-vegetation loss and fragmentation, rated on a three-point agreement scale; (iii) perceived impacts on vegetation structure, composition, and species persistence; and (iv) awareness and perceived effectiveness of the applicable policy and legal instruments. Respondents were assured of privacy and confidentiality, and participation was voluntary. Community respondents were selected by convenience sampling: adults who were available and willing to take part at the time of the survey in the wards adjacent to the park boundary were approached until the target of 20 was reached. Because a convenience sample is not statistically representative, community responses are reported descriptively and interpreted as indicative perceptions rather than population estimates. The full questionnaire is provided as Supplementary Material S1.

2.6 Data Analysis

Annual vegetation disturbance was characterized with a threshold-based index that follows the disturbance-and-persistence logic of LandTrendr [34]. Dry-season (1 May–30 September) median NDVI composites were produced for every year from 2016 to 2026 from harmonized Landsat 7 Enhanced Thematic Mapper Plus (ETM+), Landsat 8, and Landsat 9 surface-reflectance data (16–35 scenes per year for 2016–2025), with clouds and shadows masked as above. A pixel was counted as disturbed in year t when NDVI fell by more than 0.20 relative to year $t - 1$ and did not recover by

more than 0.05 in year t + 1; requiring persistence excludes transient declines caused by rainfall timing or residual cloud contamination. The thresholds were set a priori and conservatively: a fall of 0.20 in median dry-season NDVI is intended to capture only large losses of green cover rather than ordinary inter-annual variation in a multi-scene median composite, and the 0.05 recovery tolerance excludes declines that largely reverse within one year, consistent with the persistence criterion of LandTrendr-based disturbance mapping [34]. The sensitivity of the series to these values was not tested (Section 4). The disturbed area was summed within the park boundary for each year from 2017 to 2025. Because the index was not restricted to woodland pixels, it measures persistent loss of green vegetation of any type and can also respond to drought stress and to the inundation of vegetated lake margins when reservoir storage rises.

The temporal trend in the index was tested with ordinary least squares (OLS) linear regression of disturbed area against year [35]. Model significance was assessed with the F-test, residual normality with the Shapiro–Wilk test, homoscedasticity with the Breusch–Pagan test, and influence with Cook's distance; Kendall's rank correlation (τ) and a log-linear model were fitted as robustness checks. The 2017 value (1,917.5 ha, 11.2% of the park) was 1.8 times larger than that of any other year and exerted undue influence on the full-series fit (Cook's distance = 1.89, above the conventional threshold of 1). It immediately followed the 2015–2016 El Niño drought, one of the most severe in the region in several decades [36]; the subsequent recovery of reservoir storage would plausibly have inundated vegetation that had colonized the exposed lake margins, producing persistent NDVI declines unrelated to woody vegetation loss. The trend is therefore reported for 2018–2025, with the full-series result given for transparency.

To link woodland change spatially to its likely drivers, the loss rate of 2016 woodland (the proportion lost by 2025) was calculated by distance from the park boundary, a proxy for pressure from adjacent communal land, and by distance from the nearest woodland edge in 2016, a proxy for edge exposure. A logistic regression [37] of loss (1) versus persistence (0) for all 52,486 pixels of 2016 woodland was then fitted with distance to the boundary (km) and the logarithm of distance to the woodland edge as predictors. Predictive performance was evaluated as the area under the receiver operating characteristic curve (AUC) with five-fold spatial block cross-validation (1.5 km blocks), which limits the optimism caused by spatial autocorrelation. The block size was chosen to exceed the distance over which model residuals were appreciably autocorrelated: in an empirical correlogram of the residuals (6,000 randomly sampled woodland pixels), correlation fell from 0.42 at distances below 90 m to below 0.05 at 1.2–1.5 km and to approximately zero beyond 2 km. As a sensitivity check, cross-validation was repeated with 0.75, 3, and 5 km blocks, each with ten random assignments of blocks to folds. Applied to the 2025 woodland, the model gives each pixel a predicted probability of loss over a nine-year interval; pixels were classed as high risk when this probability exceeded 1.25 times the park-wide loss rate observed for 2016–2025 (17.7%), low risk when it fell below 0.75 times that rate, and medium risk otherwise. Road and settlement layers and georeferenced mining sites were not available, so the risk surface reflects boundary and edge exposure only.

Area statistics, transition matrices, landscape metrics, and the regression were computed in R version 4.6.1 (released 24 June 2026; full session information, including package versions, is provided in the supplementary material) [38] with the sf, terra, and landscapemetrics packages, and the risk model was fitted in Python with scikit-learn [39]. Questionnaire responses were coded and analyzed descriptively in the Statistical Package for the Social Sciences (SPSS). The transition-based projection of land cover to 2031 presented in the original submission was withdrawn: it had been computed over the rectangular frame rather than the park, and the transition rates observed between 2016 and 2025 are strongly influenced by reservoir-level fluctuation and by the drought-affected 2016 baseline (Section 4), so that extrapolating them would violate the stationarity assumption of transition-based projection models. The spatially explicit risk zoning described above replaces it as the study's forward-looking assessment.

3. Results

This section presents the findings of the questionnaire survey and the GIS/RS analysis undertaken to determine the key drivers and spatial extent of woody-vegetation change and fragmentation in Kyle Recreational Park.

3.1 Questionnaire Response Rate

All 50 questionnaires distributed (30 to Zimbabwe Parks and Wildlife Management Authority [ZimParks] staff and 20 to community members) were completed and returned, giving a response rate of 100%. The high response rate reflects the assurance of privacy and confidentiality given to respondents at the point of administration.

3.2 Socio-Demographic Characteristics of Park Staff

Of the 30 ZimParks staff surveyed, 19 (63.3%) were male and 11 (36.7%) were female. By age, the 31–45 cohort was the largest group (13 staff, 43.3%), followed by 18–30 (9 staff, 30%), 46–60 (7 staff, 23.3%), and 61+ (1 staff, 3.3%). Rangers made up the largest occupational group (14 staff, 46.7%), followed by administrative and support staff (8, 26.7%), general laborers (4, 13.3%), ecologists (2, 6.7%), and area managers (2, 6.7%) (Table 1, Figure 2).

Table 1. Occupational composition of Kyle Recreational Park staff (n = 30).

Occupation	Frequency	Percent (%)	Cumulative %
General laborer	4	13.3	13.3
Ranger	14	46.7	60
Ecologist	2	6.7	66.7
Admin and support staff	8	26.7	93.3
Area manager	2	6.7	100
Total	30	100	

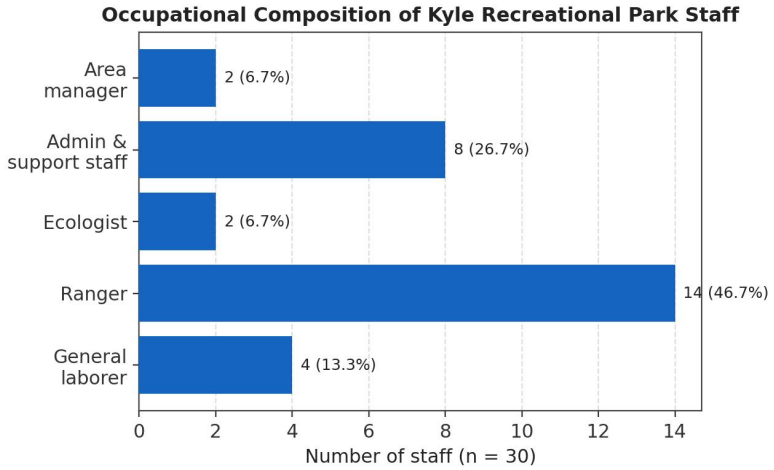

Figure 2. Occupational composition of the Kyle Recreational Park staff surveyed (n = 30), shown as the number and percentage of respondents in each occupational group.

3.3 Drivers of Woody Vegetation Loss and Fragmentation

Respondents' perceptions were broadly consistent with the image analysis in pointing to anthropogenic pressure at the park margins. A majority of respondents (52%) identified anthropogenic pressures as the principal drivers of woody-vegetation fragmentation and loss in the park, citing agricultural encroachment, logging, illegal mining, recurrent fires, and climate variability as the leading causes of habitat loss. A reduction in average forest-patch size, alongside an increase in the number of discrete patches, is itself indicative of fragmentation [40].

Respondents regarded fire as a particularly significant driver, reporting that frequent burns reduced woody cover more than infrequent ones, that the structural impact was greater in the denser granitic woodlands than in the more open basaltic landscapes, and that the effect was greatest at the park's edges; these perceptions were not tested with the imagery. By suppressing canopy formation and removing seedlings, fire reduces both the abundance and diversity of woody vegetation and can kill mature individuals of fire-sensitive species outright [41].

Table 2 summarizes staff perceptions of seven candidate drivers, rated on a three-point scale (strongly agree / agree / disagree), and these perceptions are shown graphically in Figure 3.

Table 2. Staff perceptions of drivers of woody vegetation loss and fragmentation (n = 30).

Driver	Strongly agree, n (%)	Agree, n (%)	Disagree, n (%)	No response, n (%)	Total, n (%)
Climate variability / change	7 (23.3)	10 (33.3)	13 (43.3)	0 (0.0)	30 (100)
Agricultural encroachment	6 (20.0)	12 (40.0)	12 (40.0)	0 (0.0)	30 (100)
Invasive alien species	1 (3.3)	4 (13.3)	24 (80.0)	1 (3.3)	30 (100)
Fires	15 (50.0)	13 (43.3)	2 (6.7)	0 (0.0)	30 (100)
Unsustainable exploitation	2 (6.7)	6 (20.0)	12 (40.0)	10 (33.3)	30 (100)
Illegal mining activities	5 (16.7)	2 (6.7)	13 (43.3)	10 (33.3)	30 (100)
Logging	3 (10.0)	7 (23.3)	20 (66.7)	0 (0.0)	30 (100)

Fire, illegal mining, and agricultural encroachment attracted the highest combined "strongly agree/agree" scores (Figure 3), indicating that staff perceive anthropogenic activity as the dominant proximate driver of vegetation loss, while climate variability, associated principally with drought, was identified as an important secondary, natural driver. Respondents were least persuaded that invasive alien species contribute meaningfully to woody-vegetation disturbance (80% disagreement).

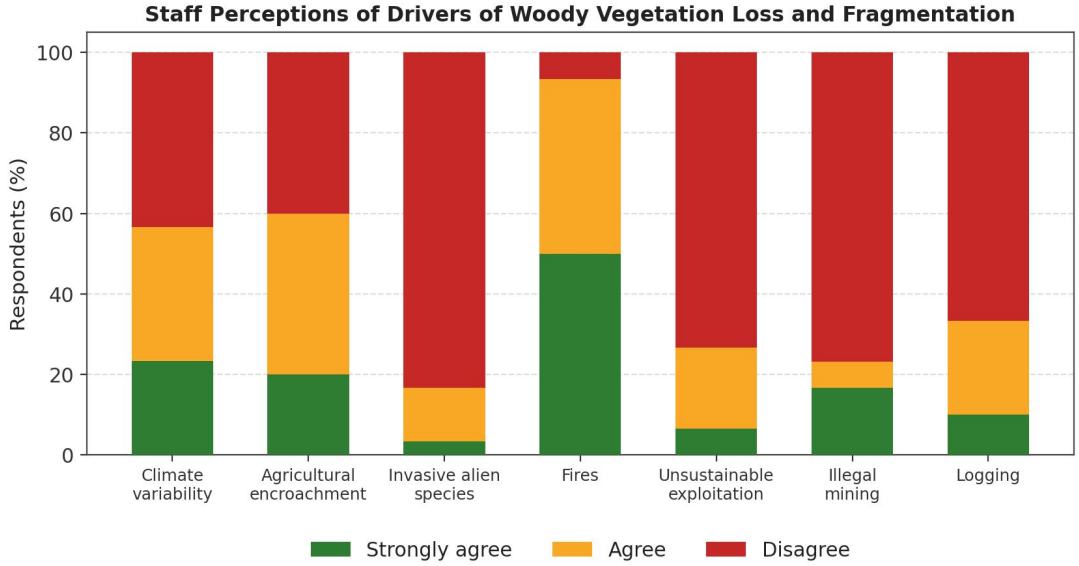

Figure 3. Staff perceptions of drivers of woody vegetation loss and fragmentation.

3.4 Policy and Legal Framework

Respondents rated the Parks and Wildlife Act, the Forest Act, and the Environmental Management Act as the most important legal instruments governing the park, each with 100% agreement on their relevance. Other instruments received more moderate recognition: the Constitution of Zimbabwe (Amendment) at 80%, the Communal Land Forest Produce Act and the National Museums and Monuments Act at 53% each, the Traditional Leaders Act at 36%, the Communal Land Act at 26%, and the Forest-Based Land Reform Policy at 23%. The Rural District Councils Act and the Forest-Based Land Reform Policy received the lowest levels of recognition, consistent with reports of weak implementation and limited compliance.

Key informants identified insufficient resourcing of implementing agencies, overlapping and poorly harmonized legislation, and limited public information as the principal deficiencies in the existing legal framework. Regarding conservation outcomes, most respondents judged existing conservation projects in the park to be broadly successful, though 16.7% disagreed and 6.7% strongly disagreed, pointing to uneven implementation across programs.

3.5 Community Perceptions

Among the 20 community members surveyed, 50% had attained tertiary education, 25% secondary education, and 10% had never attended school. A quarter of respondents had lived in the study area for more than 16 years and 30% for 11–15 years, giving many respondents direct, long-term knowledge of environmental change in and around the park; a further 10% had resided in the area for less than five years. Within this convenience sample, community respondents most often named agricultural activity and deforestation as drivers of vegetation loss, with natural fires and climate change cited less frequently (Table 3).

Table 3. Community-identified drivers of woody vegetation loss and fragmentation.

Driver	Response count	Share of responses (%)
Agricultural activities	16	39
Deforestation	12	29.3
Climate change	6	14.6
Illegal mining activities	5	12.2
Natural fires	2	4.9

Residents' perceptions of increasing fragmentation and habitat loss are consistent with the principle that a rising patch count signals active fragmentation [42]; the RS results corroborate these reports for the park margins, where woodland loss was concentrated (Section 3.9), but not for the park as a whole, where woodland patches consolidated between 2016 and 2025 (Section 3.8). Respondents also reported perceived impacts on vegetation structure and composition, and on the persistence of some plant and animal species, summarized in Table 4.

Table 4. Staff perceptions of the impacts of woody vegetation loss and fragmentation (n = 30).

Impact	Respondents, n	Share of respondents (%)
Reduction of some tree and shrub species	10	33.3
Impacts on woody vegetation structure and composition	9	30.0
Deterioration of habitat quality	6	20.0
Extinction of already-threatened species	4	13.3
No response	1	3.3
Total	30	100.0

Approximately 13.3% of respondents believe some tree species have already been lost from the park as a combined result of habitat deterioration and direct exploitation, and 30% perceived a decline in woody-vegetation structure, which they attributed to anthropogenic drivers, principally deforestation and illegal mining.

3.6 Classification Accuracy

The 2016 classification achieved an overall accuracy of 94.3% and a Kappa coefficient of 0.91, and the 2025 classification 74.6% and 0.62 (Table 5), corresponding to almost perfect and substantial agreement, respectively [43]. Woodland, the class of primary interest, was mapped reliably on both dates (producer's accuracy 80.0% and 81.8%; user's accuracy 100% and 85.7%). The lower 2025 accuracy arose mainly from confusion between open water and non-woody cover along the fluctuating lake margin: 10 of 22 water validation points were classified as non-woody, giving a producer's accuracy for water of 54.5% and a quantity disagreement of 16.4%. Open water was therefore under-mapped in 2025, and change estimates involving water are less certain than those for woodland. Because no water validation point was classified as woodland and no woodland point as water, this error affects the water and non-woody estimates but not the woodland estimates. Its possible magnitude can be bounded indicatively: if the omission rate for water in the validation sample (45.5%) applied across the whole lake surface, about 2,800 ha of open water would have been mapped as non-woody in 2025. The 2025 non-woody area (7,498.6 ha) would then be overestimated by up to that amount, the net decline in non-woody cover (−2,087.6 ha) understated (up to about −4,900 ha), and the net gain in water (+859.7 ha) understated (up to about +3,700 ha). Because the validation points were not a probability sample, this is an upper-bound illustration rather than an area-adjusted estimate. In 2016, three of 15 woodland validation points were classified as non-woody, indicating slight under-mapping of woodland in that year.

Table 5. Confusion matrices and accuracy measures for the 2016 and 2025 classifications (withheld validation points).

Reference\Classified	Woodland	Non-woody	Water	Total	Producer's accuracy (%)
2016 (validation points, n = 53)					
Woodland	12	3	0	15	80.0
Non-woody	0	26	0	26	100.0
Water	0	0	12	12	100.0
Total	12	29	12	53	
User's accuracy (%)	100.0	89.7	100.0		
Overall accuracy 94.3%; Kappa 0.91; quantity disagreement 5.7%; allocation disagreement -0.0%					
2025 (validation points, n = 67)					
Woodland	18	4	0	22	81.8
Non-woody	3	20	0	23	87.0
Water	0	10	12	22	54.5
Total	21	34	12	67	
User's accuracy (%)	85.7	58.8	100.0		
Overall accuracy 74.6%; Kappa 0.62; quantity disagreement 16.4%; allocation disagreement 9.0%.					

3.7 Land-Cover Change and Gross Woodland Dynamics, 2016–2025

Within the park boundary, woodland increased from 4,723.7 ha (28.0% of the mapped area) in 2016 to 6,051.2 ha (35.7%) in 2025, a net gain of 1,327.4 ha (+28.1%) (Table 6, Figure 4). Non-woody cover declined by 2,087.6 ha (−21.8%), and mapped open water increased by 859.7 ha (+33.9%). Mapped open water (2,533.9 ha in 2016 and 3,393.5 ha in 2025) was far below the full-supply lake area given in Section 2.1, showing that the reservoir was drawn down on both dates; exposed lakebed and the herbaceous vegetation colonizing it were therefore mapped as non-woody. The mapped total was 16,843.9 ha in 2016 and 16,943.3 ha in 2025, slightly below the 17,071.8 ha boundary area because pixels straddling the boundary were excluded and, in 2016, because 99.5 ha of the lake surface had no cloud-free observation.

Table 6. Land-cover area and net change within Kyle Recreational Park, 2016–2025.

Class	2016 (ha)	2016 (%)	2025 (ha)	2025 (%)	Net change (ha)	Net change (%)
Woodland	4,723.74	28.0	6,051.15	35.7	+1,327.41	+28.1
Non-woody	9,586.26	56.9	7,498.62	44.3	−2,087.64	−21.8
Water	2,533.86	15.0	3,393.54	20.0	+859.68	+33.9
Total mapped	16,843.86	100.0	16,943.31	100.0	+99.45	

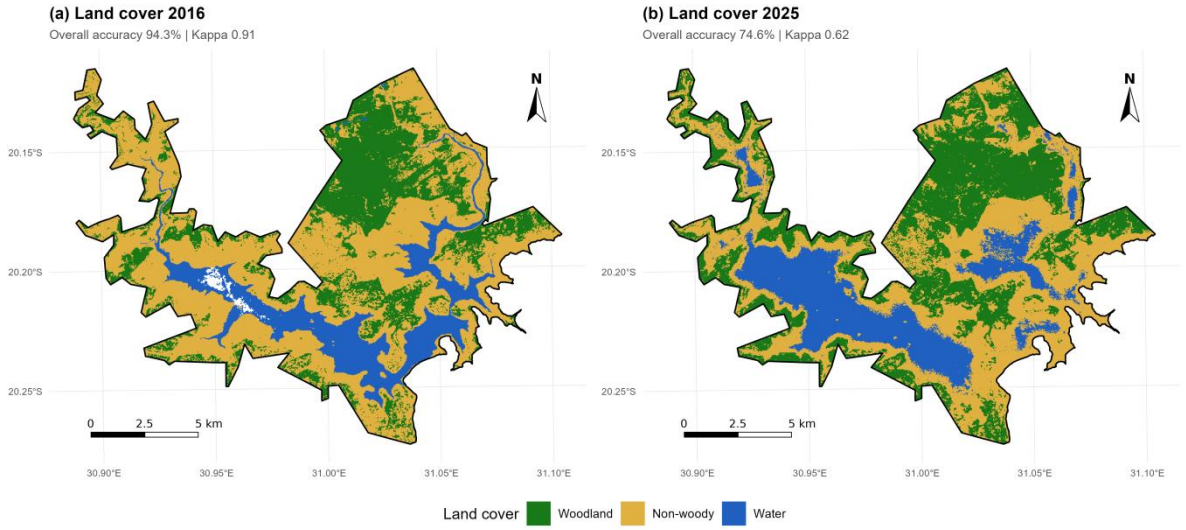

Figure 4. Land cover of Kyle Recreational Park in (a) 2016 and (b) 2025, classified from dry- and wet-season Landsat composites and masked to the park boundary. White areas within the 2016 boundary lack cloud-free observations. Projection: WGS 84 / UTM zone 36S.

Gross woodland change. The net woodland gain concealed substantial turnover (Table 7). Between 2016 and 2025, 834.0 ha of woodland were lost (829.1 ha to non-woody cover and 5.0 ha to water) and 2,161.4 ha were gained, all from non-woody cover, resulting in a net increase of 1,327.4 ha. Thus 17.7% of the 2016 woodland had been lost by 2025, and 35.7% of the 2025 woodland was new. Across all classes, 5,610.5 ha (33.3%) of the area mapped on both dates changed class, of which 3,522.9 ha (62.8%) was swap change, that is, gains in one place offset by losses of the same class elsewhere. The exchanges between non-woody cover and water (1,685.2 ha of non-woody to water and 929.9 ha of water to non-woody) largely reflect differences in reservoir level between the two dates rather than land-cover conversion. Excluding every pixel mapped as water on either date, 2,990.5 ha (23.7%) of the 12,619.7 ha of terrestrial land changed class (829.1 ha from woodland to non-woody and 2,161.4 ha from non-woody to woodland, a woodland–non-woody swap of 1,658.2 ha). Transitions involving water therefore account for 2,620.0 ha (46.7%) of all mapped change, and the terrestrial figure of 23.7% is the better measure of vegetation turnover. Woodland loss occurred throughout the park but was most extensive along the northern boundary, in the eastern arm, and in the southern section, whereas gains were widespread in the northern-shore woodland and along the western arms (Figure 5).

Table 7. Transition matrix (ha) between 2016 (rows) and 2025 (columns), with gross gain, gross loss, net change, and swap change for each class.

2016 \ 2025	Woodland	Non-woody	Water	Total 2016	Gross loss
Woodland	3,889.71	829.08	4.95	4,723.74	834.03
Non-woody	2,161.44	5,739.48	1,685.16	9,586.08	3,846.60
Water	0.00	929.88	1,603.98	2,533.86	929.88
Total 2025	6,051.15	7,498.44	3,294.09	16,843.68	
Gross gain	2,161.44	1,758.96	1,690.11		
Net change	+1,327.41	−2,087.64	+760.23		
Swap change	1,668.06	3,517.92	1,859.76		

Note: Values refer to the 16,843.7 ha mapped on both dates; 99.5 ha of lake surface without a cloud-free 2016 observation are excluded, which explains the difference in net water change from Table 6.

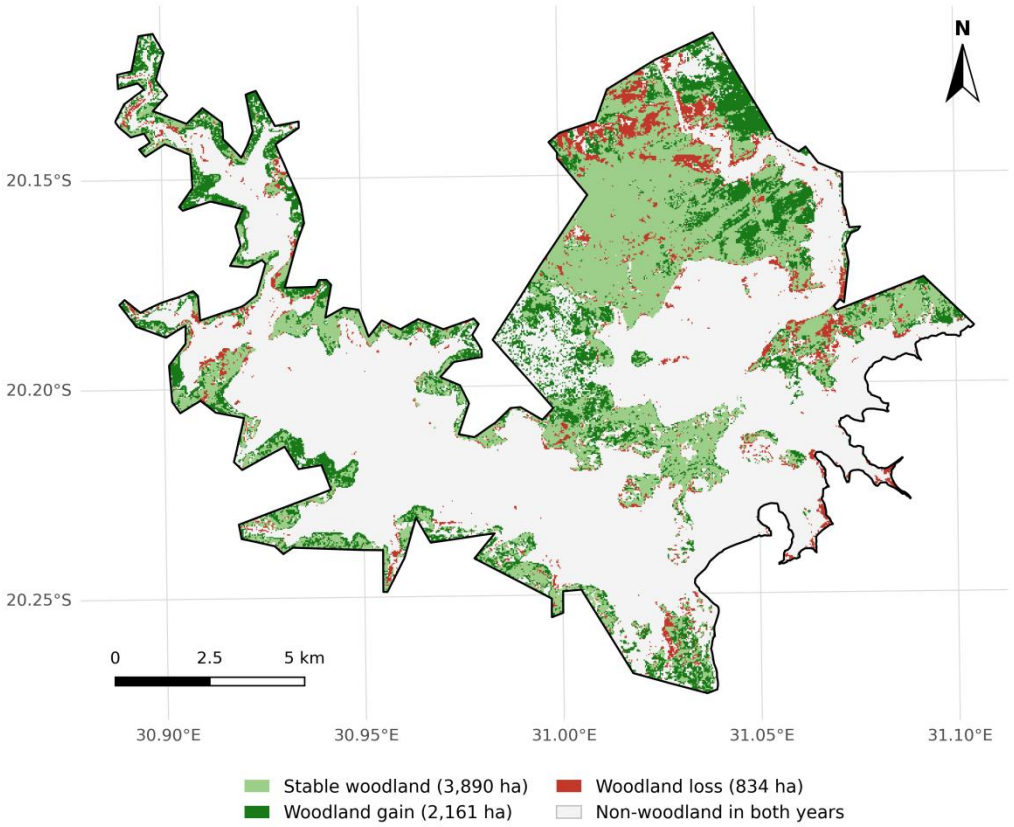

Figure 5. Woodland change in Kyle Recreational Park between 2016 and 2025, showing stable woodland, woodland gain, and woodland loss; light grey denotes areas that were non-woodland on both dates. Projection: WGS 84/UTM zone 36S.

3.8 Woodland Fragmentation

Woodland structure changed markedly between 2016 and 2025 (Table 8). The number of woodland patches fell by 57.0%, from 1,117 to 480, and patch density fell from 7.81 to 3.54 patches per 100 ha, while mean patch size nearly tripled, from 4.23 ha to 12.61 ha. Edge density declined by 9.1%, the largest patch index rose from 15.4% to 18.6%, and total core area increased by 44.8%, from 2,939.6 ha to 4,256.6 ha (62.2% and 70.3% of woodland area, respectively). Together these changes describe consolidation of the woodland matrix, as gains filled gaps between and around existing patches, rather than the increase in patch number and decline in patch size that characterize active fragmentation. The landscape-level metrics therefore do not support the proposition that woodland in the park as a whole became more fragmented between 2016 and 2025; fragmentation was instead localized at woodland edges and near the park boundary (Section 3.9).

Table 8. Class-level fragmentation metrics for woodland, Kyle Recreational Park, 2016 and 2025 (terrestrial landscape; eight-neighbour rule; edge depth 30 m).

Metric	2016	2025	Change	Change (%)
Class area, CA (ha)	4,723.74	6,051.15	+1,327.41	+28.1
Number of patches, NP	1,117	480	−637	−57.0
Patch density, PD (patches per 100 ha)	7.81	3.54	−4.26	−54.6
Mean patch size, MPS (ha)	4.23	12.61	+8.38	+198.1
Edge density, ED (m ha−1)	67.09	60.99	−6.11	−9.1
Largest patch index, LPI (%)	15.39	18.60	+3.21	+20.8
Total core area, TCA (ha)	2,939.58	4,256.64	+1,317.06	+44.8
Core area as share of CA (%)	62.2	70.3	+8.1	+13.0

3.9 Spatial Pattern of Woodland Loss and Future Risk Zones

Woodland loss was strongly structured in space (Table 9; Figure 6b, 6c). Within 1 km of the park boundary, 21.6% of the 2016 woodland was lost, compared with 13.8% further inside; this zone held 49.6% of the 2016 woodland but accounted for 60.8% of all woodland loss. Loss rates remained above 20% up to 1.5 km from the boundary and then fell to 12.7% at 1.5–2.5 km and 7.3% beyond 2.5 km. Exposure at woodland edges had a similar effect: 25.3% of woodland pixels at a patch edge (within 30 m of non-woodland) were lost, compared with 16.0% at 31–60 m, 14.0% at 61–120 m, and 10.3%

more than 120 m from an edge. The zone within 500 m of the boundary also recorded the largest woodland gain (1,181.6 ha), indicating that the park margin is the most dynamic part of the landscape, with both clearance and regrowth.

Table 9. Woodland loss and gain, 2016–2025, by distance from the park boundary.

Distance from boundary	Woodland 2016 (ha)	Woodland lost (ha)	Loss rate (%)	Share of total loss (%)	Woodland gained (ha)
0–500 m	1,520.64	331.20	21.8	39.7	1,181.61
500–1,000 m	822.87	175.50	21.3	21.0	363.78
> 1,000 m	2,380.23	327.33	13.8	39.2	616.05
Total	4,723.74	834.03	17.7	100.0	2,161.44

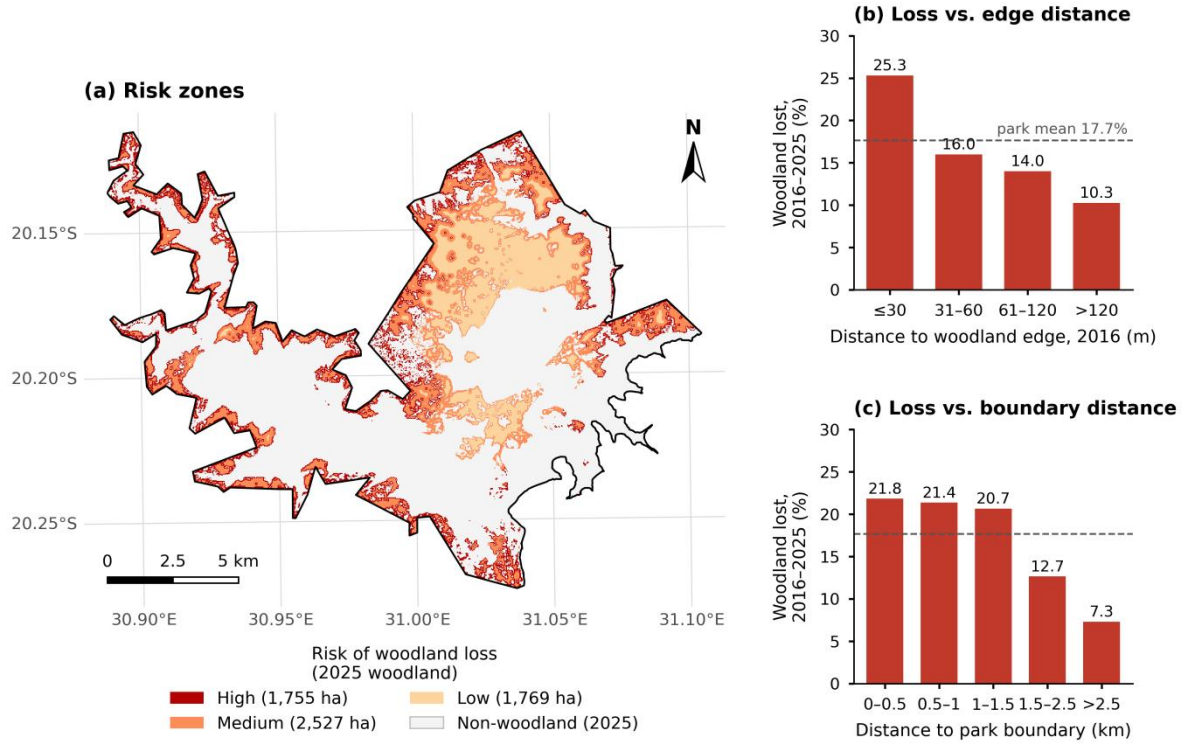

Figure 6. Future risk of woodland loss in Kyle Recreational Park. (a) Risk zones for the 2025 woodland, derived from a logistic model of 2016–2025 woodland loss with distance to the park boundary and distance to the woodland edge as predictors (high: predicted nine-year loss probability > 22.1%; medium: 13.2%–22.1%; low: < 13.2%). (b, c) Observed proportion of 2016 woodland lost by 2025 by distance to the nearest woodland edge in 2016 and by distance to the park boundary; the dashed line marks the park-wide loss rate (17.7%).

In the logistic model, the odds of loss decreased by 27% for each additional kilometre from the park boundary (odds ratio 0.73) and by about 28% for each doubling of the distance from the woodland edge (odds ratio 0.72). Spatially cross-validated discrimination was modest (mean AUC = 0.62; range 0.53–0.72 across folds; in-sample AUC = 0.64); with larger blocks that exceed the residual autocorrelation range, mean AUC was 0.59 (3 km blocks) and 0.60 (5 km blocks), ranging from 0.53 to 0.63 across the ten fold assignments, which is expected for a model with two distance predictors and means that the zones indicate relative rather than absolute risk. Applied to the 2025 woodland, the model placed 1,754.6 ha (29.0%) in the high-risk zone, 2,527.3 ha (41.8%) in the medium-risk zone, and 1,769.2 ha (29.2%) in the low-risk zone (Figure 6a). High-risk woodland forms a near-continuous belt along the outer boundary, the narrow western arms, the eastern arm, and the southern section, and also fringes woodland patches in the interior, whereas low-risk woodland is largely confined to the interior of the large woodland blocks on the northern shore.

3.10 Temporal Trend in Vegetation Disturbance, 2017–2025

The annual area of persistent vegetation decline ranged from 18.5 ha (2019) to 1,038.8 ha (2024) over 2018–2025 and increased significantly over this period (Figure 7). The fitted OLS model was $y = 324.8 + 115.9(t - 2021.5)$, where y is the annual area of persistent NDVI decline (ha) and t is the calendar year (95% confidence interval for the slope: 26.3–205.5 ha yr^{-1}; $R^2 = 0.63$; adjusted $R^2 = 0.56$; $F(1, 6) = 10.02$; $p = 0.019$). The confidence interval is wide because the series is short (eight annual values, leaving six residual degrees of freedom) and inter-annual variability is large; the direction of the trend is therefore better supported than its magnitude. Residuals were consistent with normality (Shapiro–Wilk $p = 0.76$) and homoscedasticity (Breusch–Pagan $p = 0.21$), and no observation was unduly influential (maximum

Cook's distance = 0.83, for 2024). The trend was confirmed by Kendall's rank correlation ($\tau = 0.64$; $p = 0.031$) and by a log-linear model ($p = 0.008$). With 2017 included, the series showed no trend (slope = −25.0 ha yr^{-1}; $R^2 = 0.01$; $F(1, 7) = 0.08$; $p = 0.78$), because the single 2017 value dominated the fit. The null hypothesis of no temporal trend in persistent vegetation decline is therefore rejected for 2018–2025. The three highest values after 2017 occurred in 2023–2025, and the 2024 peak coincided with the 2023–2024 El Niño drought, which caused severe rainfall deficits across Zimbabwe [44]; part of the upward trend therefore reflects drought stress rather than anthropogenic disturbance alone.

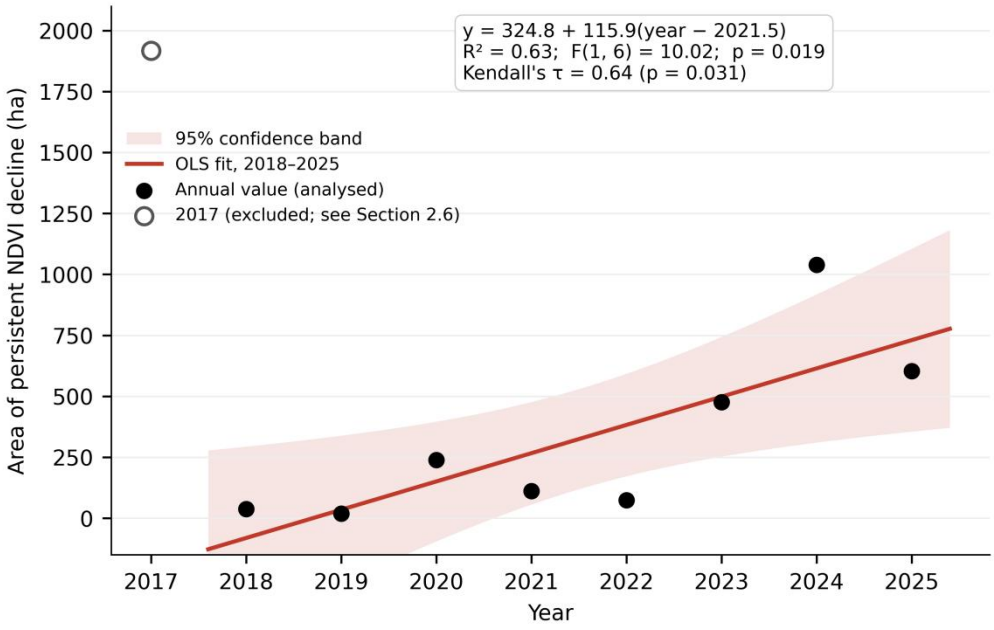

Figure 7. Annual area of persistent vegetation decline (NDVI decrease > 0.20 not recovered in the following year) within Kyle Recreational Park, with the OLS trend for 2018–2025 and its 95% confidence band. The 2017 value (open circle) is shown but excluded from the fit (Section 2.6).

4. Discussion

Analysis of the 2016 and 2025 imagery reveals two concurrent trajectories that become apparent only because change was assessed as gross as well as net change, and at the patch as well as the class level: a net expansion and consolidation of woodland across the park, and persistent, spatially concentrated loss at woodland edges and near the park boundary, where 17.7% of the 2016 woodland was lost within nine years. This edge-concentrated loss is consistent with the perceptions of community respondents, a quarter of whom had lived in the area for more than 16 years and who reported declining cover and increasing fragmentation in specific locations, especially the park margins; because these perceptions come from a small convenience sample, they are treated as indicative only. This pattern is consistent with the broader finding that vegetation loss shifts species composition and evenness [3,45]: as woody cover contracts locally, small-statured, herbaceous species tend to proliferate at the expense of larger trees, because deforestation preferentially removes larger individuals sought for socio-economic use [46].

A likely explanation for the apparent paradox of a 28.1% net increase in woodland cover occurring alongside localized loss is bush encroachment, the progressive thickening of woody plants that is widespread across southern African savannas [47,48]. Rising atmospheric carbon dioxide, altered fire regimes, and heavy grazing of grasslands favor the recruitment and densification of shrubs and small trees, so that mapped "woodland" area can expand rapidly even as large, mature canopy trees are selectively removed at the park edges [47,49]. The conversion of 2,161 ha of non-woody cover to woodland, and the infilling of gaps that more than halved the number of woodland patches, are consistent with this process [48]. Two further factors are likely to have inflated the mapped gain. First, the 2016 baseline followed the 2015–2016 El Niño drought [36]; drought-stressed woody canopies with reduced dry-season greenness are more easily confused with non-woody cover, and the 2016 validation indicated some under-mapping of woodland (producer's accuracy 80%), so part of the apparent gain may represent recovery of canopy condition rather than new woody cover. Second, woody plants can colonize lake margins that remain exposed during prolonged reservoir drawdown, which may explain some of the gains along the western arms. Encroached thicket is not ecologically equivalent to mature woodland: it typically supports lower structural diversity and different faunal assemblages, so the mapped gain should not be read as an equivalent gain in mature woodland habitat. Because the woodland class could not be verified floristically in the field (Section 2.2), plot-based surveys that distinguish mature woodland from encroached thicket are a priority for future work.

Respondents attributed much of the perceived increase in deforestation to fuelwood demand from surrounding communities and reported that land clearance for agriculture had converted some woodland to shrubland at the park's edges, consistent with the well-established link between agricultural expansion, habitat fragmentation, and declining

species richness and evenness [50]. In respondents' views, agricultural encroachment, illegal mining, and climate variability account for most of the fragmentation, and some respondents believed that locally valued woody species have already been lost from parts of the park; these reports could not be verified with the imagery. This is consistent with the broader literature on fragmentation: once continuous habitat is cleared for agriculture or other intensive use, the residual fragments behave as isolated "habitat islands" separated by farmland and pasture [51,52], and fragmentation together with outright habitat loss remains among the most serious global threats to biodiversity.

Fragmentation also operates through structural edge effects that extend well beyond the cleared area itself. Newly created woodland edges experience elevated temperatures, reduced humidity, increased wind exposure, and higher light penetration, which alter microclimates, elevate tree mortality, and favor disturbance-tolerant and pioneer species over forest-interior specialists [45]. The loss gradient observed here is consistent with this mechanism: woodland at patch edges was lost at 2.5 times the rate of woodland more than 120 m from an edge. Two implications follow for this study. First, edge-driven degradation means that the ecological loss associated with fragmentation exceeds what class-area statistics alone capture. Second, edge effects can distort biodiversity indexing: species counts made in edge-influenced fragments may remain stable or even rise (through an influx of generalists) while interior-dependent woodland species decline, so richness measures should be interpreted alongside composition and the core-area metric reported in Table 8, which shows that core woodland area increased even as loss continued at the margins.

Respondents also associated human disturbance with reduced densities of economically valuable timber species and implicated both natural and anthropogenic fire, including fires linked to poaching activity, arson, and logging; they judged areas with high litter loads to be at greatest risk given the availability of fuel. This is consistent with evidence that human encroachment around protected areas increases fire frequency [53], and that fires are sometimes deliberately set or rekindled by poachers from neighboring communities and resettlement areas as a trapping method [54].

The regression of the annual area of persistent vegetation decline against time showed a significant increase between 2018 and 2025 ($R^2 = 0.63$; $F(1, 6) = 10.02$; $p = 0.019$), so the null hypothesis of no temporal trend is rejected for this period. The trend should nonetheless be interpreted cautiously: the series is short (eight years), the index includes non-woody vegetation, and its highest values coincided with the 2023–2024 El Niño drought [44], so drought stress and anthropogenic disturbance cannot be fully separated. Taken together with the net expansion and consolidation of woodland cover recorded between 2016 and 2025, the most defensible interpretation is that the park's vegetation trajectory reflects two concurrent processes: continued anthropogenic pressure concentrated at the park margins and woodland edges, and woody encroachment and post-drought recovery across larger areas of the park interior.

From a management perspective, the findings support several complementary interventions. Foremost, because edge-boundary exploitation is driven by household economic dependence on woodland resources, community-led co-management offers greater long-term protection than punitive enforcement alone. Collaborative arrangements in Zimbabwe's Communal Areas Management Programme for Indigenous Resources (CAMPFIRE) tradition, in which adjacent communities share tangible benefits from, and responsibility for, park resources, directly address the underlying driver rather than its symptoms [55]. The risk zoning shows where such arrangements should be concentrated: high-risk woodland (1,755 ha) lies predominantly within about 1.5 km of the boundary and along woodland edges, so boundary patrols, firebreak maintenance, and community agreements can be targeted to a well-defined belt rather than spread across the whole park. Complementary measures include: (i) defining and maintaining ecologically appropriate woody-vegetation densities for each protected area, consistent with sustainable carrying capacity, including active management of bush encroachment where thickening displaces grassland; (ii) sustaining long-term monitoring and research programs tracking vegetation structure and composition [56]; and (iii) closer collaboration between the Environmental Management Agency (EMA), ZimParks, the Forestry Commission, and traditional leadership structures on joint awareness campaigns and alternative-livelihood programs (e.g., woodlots, improved cookstoves, and beekeeping) that reduce dependence on in-park resources. Enforcement of existing law remains necessary, particularly against illegal mining, but is positioned here as a complement to, not a substitute for, co-management.

Several limitations qualify these findings. First, cropland, grassland, and rock outcrop could not be separated reliably at 30 m resolution and were merged into a single non-woody class, so agricultural expansion within the park could not be quantified directly. Second, accuracy was lower in 2025 than in 2016, mainly because water was confused with non-woody cover along the fluctuating shoreline; estimates for woodland, mapped with producer's and user's accuracies above 80% on both dates, are more reliable than those for water. A stable water mask derived from the reservoir's full-supply extent, applied as a post-classification constraint, or a separate class for exposed lakebed, would probably have absorbed most of this error and is recommended for future work. Third, reference points were placed by image interpretation rather than by probability sampling, which precludes area-adjusted accuracy estimates [29], and the validation samples were small ($n = 53$ and $n = 67$). Fourth, a comparison of two single-year composites is sensitive to inter-annual climate, and the drought-affected 2016 baseline probably inflated the apparent woodland gain; multi-year baseline composites would reduce this effect. Fifth, no minimum mapping unit was applied, so isolated misclassified pixels may have inflated the 2016 patch count. Finally, the disturbance index is a threshold-based approximation rather than a full LandTrendr segmentation, was not restricted to woodland, and was not tested for sensitivity to its thresholds, and the risk model uses distance predictors only; road, settlement, and mining-site data would sharpen the attribution of loss to specific drivers.

5. Conclusions and Recommendations

This study set out to identify the key drivers of woody-vegetation change and fragmentation in Kyle Recreational Park and to map its spatial extent between 2016 and 2025. Woodland cover increased by 28.1% (net 1,327 ha) and became more consolidated, yet 834 ha (17.7%) of the 2016 woodland was lost, with loss concentrated within about 1.5 km of the park boundary and at woodland edges, and the annual area of persistent vegetation decline increased between 2018 and 2025. The evidence indicates that human encroachment has contributed substantially to localized deterioration of woodland condition, even as overall woodland cover expanded at the landscape scale, a pattern consistent with woody encroachment and post-drought recovery operating alongside edge-concentrated loss. Combining RS with a structured questionnaire survey allowed the two data sources to be compared: the imagery shows loss concentrated at the park margins, and respondents, whose views are indicative rather than representative, attributed this loss primarily to deforestation linked to logging, agricultural expansion, and illegal mining, compounded by drought and fire. Respondents identified Mopane and Combretum (locally, "Mutsviri") as among the most heavily affected species, which they linked to their socio-economic value and exposure to selective harvesting; this perception could not be independently verified with the imagery and warrants plot-based follow-up.

Limited integration of local and traditional institutions into woodland governance appears to be a structural driver of degradation: local government agencies are heavily oriented toward agricultural extension services, with comparatively little capacity directed at forest management or the land-use implications of woodland loss. We recommend that woodland management be formally integrated into state extension programming in partnership with traditional institutions, and that the national forest policy be strengthened and mainstreamed into national accounting and reporting systems, supported by a comprehensive communication, education, and public-awareness strategy for sustainable forest use.

Specifically, the study recommends:

(1) Establishment of community-led co-management arrangements, in partnership with traditional leadership, that give boundary communities tangible benefits from park resources and reduce household economic dependence on in-park fuelwood, timber, arable land, and minerals, complemented by alternative-livelihood support (woodlots, improved cookstoves, and apiculture).

(2) Active management of bush encroachment and of grassland–woodland balance, including protection of remaining mature woodland pockets, rehabilitation of degraded grassland, and stream-bank buffering.

(3) Targeted intervention against the specific edge-fragmentation drivers identified here (agricultural encroachment, illegal mining, and fire) in the 1,755 ha of high-risk woodland mapped in Section 3.9 (Figure 6), which lies predominantly within 1.5 km of the park boundary and along woodland edges.

(4) Continuous, systematic monitoring of anthropogenic activity, vegetation structure, and fragmentation metrics, supported by regular RS updates based on multi-year composites, probability-based accuracy assessment, and ground-referenced disturbance records.

(5) Enforcement of existing legislation, particularly the Parks and Wildlife Act, Forest Act, and Environmental Management Act, together with harmonization of overlapping legal instruments and increased resourcing for implementing agencies, as a complement to co-management.

(6) Further research on woodland structure, composition, and livelihoods in Kyle Recreational Park, to clarify the interactions between the woodland resource, its users, and the institutions that mediate access to it, including separation of cropland, grassland, and bare surfaces with higher-resolution imagery (e.g., Sentinel-2) and georeferencing of mining and settlement sites.

Acknowledgements

The authors thank Gwanda State University for providing working space and internet access.

Funding

This research received no external funding.

Ethics Statement

The questionnaire survey was designed and conducted by the authors as independent research before they joined Gwanda State University, and the data were collected under a research permit issued by ZimParks, the authority responsible for the park. The University's involvement began after data collection and was limited to providing working space and internet access; the study was therefore not submitted to, or reviewed by, the University's research ethics committee, and no institutional ethics approval number is available. The survey followed standard ethical principles for research with

human participants: only consenting adults took part, participation was voluntary, responses were anonymous, and no sensitive personal data were collected.

Informed Consent

All respondents were informed of the purpose of the study, assured of privacy and confidentiality, and participated voluntarily; consent was obtained prior to questionnaire administration.

Data Availability Statement

The classified land-cover maps, the woodland-change and risk-zone rasters, the annual disturbance series, and the GEE, R, and Python scripts used in this study, together with the R session information listing all package versions, are provided as supplementary material; the anonymised questionnaire responses are available from the corresponding author on reasonable request.

Author Contributions

Conceptualization, E.T.; methodology, E.T. and F.B.; formal analysis, E.T.; investigation, E.T. and F.B.; writing–original draft preparation, E.T.; writing–review and editing. All authors have read and agreed to the published version of the manuscript.

Conflict of Interest

The authors declare no conflict of interest.

Generative AI Statement

During revision, a generative artificial-intelligence assistant (Grammarly) was used to assist with language editing, Claude was used in drafting of analysis code (GEE, R, and Python), statistical analysis of the disturbance series and the risk model, and preparation of maps and figures. All analyses were run on the authors' data, and the authors reviewed and verified all code, results, and text and take full responsibility for the integrity of the work.

References

[1] Tiscornia G, Jaurena M, Baethgen W. Drivers, process, and consequences of native grassland degradation: insights from a literature review and a survey in Río de la Plata grasslands. Agronomy, 2019, 9(5), 239. DOI: 10.3390/agronomy9050239

[2] Chapungu L, Nyamadzawo G, Zinhiva H. A multi-method analysis of forest fragmentation and loss: The case of Ward 11, Chiredzi District, Zimbabwe. African Journal of Environmental Science and Technology, 2014, 8(2), 121-128. DOI: 10.5897/AJEST2013.1556

[3] Aguilar-Santelises R, del Castillo RF. Factors affecting woody plant species diversity of fragmented seasonally dry oak forests in the Mixteca Alta, Oaxaca, Mexico. Revista Mexicana de Biodiversidad, 2013, 84(2), 575-590. DOI: 10.7550/rmb.30458

[4] Laverty MF, Gibbs JP. Ecosystem loss and fragmentation: Synthesis. Lessons in Conservation, 2007, 1, 72-96. New York: Network of Conservation Educators and Practitioners, American Museum of Natural History.

[5] Intergovernmental Panel on Climate Change (IPCC). Climate change 2022–Impacts, adaptation and vulnerability: contribution of Working Group II to the Sixth Assessment Report of the Intergovernmental Panel on Climate Change. Cambridge, UK: Cambridge University Press, 2022. DOI: 10.1017/9781009325844

[6] Myhre G, Shindell D, Bréon FM, Collins W, Fuglestvedt J, Huang J, et al. Anthropogenic and natural radiative forcing. In: Climate Change 2013: The Physical Science Basis. Contribution of Working Group I to the Fifth Assessment Report of the IPCC. Cambridge, UK: Cambridge University Press, 2013.

[7] Martin RE, Sapsis DB. Fires as agents of biodiversity: Pyrodiversity promotes biodiversity. In: Proceedings of the Symposium on Biodiversity of Northwestern California, 1992.

[8] van der Werf GR, Randerson JT, Giglio L, Collatz GJ, Mu M, Kasibhatla PS, et al. Global fire emissions and the contribution of deforestation, savanna, forest, agricultural, and peat fires (1997–2009). Atmospheric Chemistry and Physics, 2010, 10(23), 11707-11735. DOI: 10.5194/acp-10-11707-2010

[9] Scholes RJ, Archibald S, von Maltitz G. Emissions from fire in sub-Saharan Africa: The magnitude of sources, their variability, and uncertainty. Global Environmental Research, 2011, 15, 53-63.

[10] Archibald S, Lehmann CER, Gómez-Dans JL, Bradstock RA. Defining pyromes and global syndromes of fire regimes. Proceedings of the National Academy of Sciences, 2013, 110(16), 6442-6447. DOI: 10.1073/pnas.1211466110

[11] Government of the Republic of Zimbabwe. Zimbabwe's fourth national report to the Convention on Biological Diversity. Harare: Ministry of Environment and Natural Resources Management, 2010.

[12] Chibememe G, Muboko N, Gandiwa E, Kupika OL, Muposhi VK, Pwiti G. Embracing indigenous knowledge systems in the management of dryland ecosystems in the Great Limpopo Transfrontier Conservation Area: The case of Chibememe and Tshovani communities, Chiredzi, Zimbabwe. Biodiversity, 2014, 15(2-3), 192-201. DOI: 10.1080/14888386.2014.934715

[13] Biggs D, Courchamp F, Martin R, Possingham HP. Legal trade of Africa's rhino horns. Science, 2013, 339(6123), 1038-1039. DOI: 10.1126/science.1229998

[14] Munowenyu EM. Advanced level geography: A Comprehensive Guide. Harare: Longman Zimbabwe, 1996.

[15] Chenje M, Sola L, Paleczny D (Eds.). The state of Zimbabwe's environment 1998. Harare: Government of the Republic of Zimbabwe, Ministry of Mines, Environment and Tourism, 1998.
[16] Mukwashi K. Influence of elephant (*Loxodonta africana Blumenbach*) on *Baikiaea plurijuga* dominated woody vegetation around natural and artificial watering points in the northern part of Hwange National Park, Zimbabwe. MSc thesis, University of Zimbabwe, Harare, 2006.
[17] Mutowo G, Mutanga O, Masocha M. Evaluating the applications of the near-infrared region in mapping foliar N in the Miombo woodlands. Remote Sensing, 2018, 10(4), 505. DOI: 10.3390/rs10040505
[18] Pikirayi I. The Zimbabwe Culture: Origins and Decline of Southern Zambezian States. Walnut Creek, CA: AltaMira Press, 2001.
[19] Natural Earth. 1:10m cultural vectors: Admin 0–countries; Admin 1–states, provinces; populated places. Available from: https://www.naturalearthdata.com (accessed on 28 September 2026).
[20] Gorelick N, Hancher M, Dixon M, Ilyushchenko S, Thau D, Moore R. Google Earth Engine: Planetary-scale geospatial analysis for everyone. Remote Sensing of Environment, 2017, 202, 18-27. DOI: 10.1016/j.rse.2017.06.031
[21] Sidhu N, Pebesma E, Camara G. Using Google Earth Engine to detect land cover change: Singapore as a use case. European Journal of Remote Sensing, 2018, 51(1), 486-500. DOI: 10.1080/22797254.2018.1451782
[22] McFeeters SK. The use of the Normalized Difference Water Index (NDWI) in the delineation of open water features. International Journal of Remote Sensing, 1996, 17(7), 1425-1432. DOI: 10.1080/01431169608948714
[23] Huete AR. A soil-adjusted vegetation index (SAVI). Remote Sensing of Environment, 1988, 25(3), 295-309. DOI: 10.1016/0034-4257(88)90106-X
[24] Farr TG, Rosen PA, Caro E, Crippen R, Duren R, Hensley S, et al. The shuttle radar topography mission. Reviews of Geophysics, 2007, 45(2), RG2004. DOI: 10.1029/2005RG000183
[25] Breiman L. Random forests. Machine Learning, 2001, 45(1), 5-32. DOI: 10.1023/A:1010933404324
[26] Pontius Jr RG, Shusas E, McEachern M. Detecting important categorical land changes while accounting for persistence. Agriculture, Ecosystems & Environment, 2004, 101(2-3), 251-268. DOI: 10.1016/j.agee.2003.09.008
[27] Næsset E. Use of the weighted Kappa coefficient in classification error assessment of thematic maps. International Journal of Geographical Information Systems, 1996, 10(5), 591-603. DOI: 10.1080/02693799608902099
[28] Pontius Jr RG, Millones M. Death to Kappa: Birth of quantity disagreement and allocation disagreement for accuracy assessment. International Journal of Remote Sensing, 2011, 32(15), 4407-4429. DOI: 10.1080/01431161.2011.552923
[29] Olofsson P, Foody GM, Herold M, Stehman SV, Woodcock CE, Wulder MA. Good practices for estimating area and assessing accuracy of land change. Remote Sensing of Environment, 2014, 148, 42-57. DOI: 10.1016/j.rse.2014.02.015
[30] Hesselbarth MHK, Sciaini M, With KA, Wiegand K, Nowosad J. landscapemetrics: An open-source R tool to calculate landscape metrics. Ecography, 2019, 42(10), 1648-1657. DOI: 10.1111/ecog.04617
[31] McGarigal K, Cushman SA, Ene E. FRAGSTATS v4: Spatial pattern analysis program for categorical and continuous maps. Amherst, MA: University of Massachusetts, 2012.
[32] Bulmer M. Questionnaires: An introduction. In: Bulmer M (Ed.), Questionnaires (Vol. 1). London: Sage, 2004.
[33] Jones TL, Baxter MAJ, Khanduja V. A quick guide to survey research. Annals of the Royal College of Surgeons of England, 2013, 95(1), 5-7. DOI: 10.1308/003588413X13511609956372
[34] Kennedy RE, Yang Z, Cohen WB. Detecting trends in forest disturbance and recovery using yearly Landsat time series: 1. LandTrendr temporal segmentation algorithms. Remote Sensing of Environment, 2010, 114(12), 2897-2910. DOI: 10.1016/j.rse.2010.07.008
[35] Montgomery DC, Peck EA, Vining GG. Introduction to Linear Regression Analysis. 6th ed. Hoboken, NJ: Wiley, 2021.
[36] Archer ERM, Landman WA, Tadross MA, Malherbe J, Weepener H, Maluleke P, Marumbwa FM. Understanding the evolution of the 2014–2016 summer rainfall seasons in southern Africa: key lessons. Climate Risk Management, 2017, 16, 22-28. DOI: 10.1016/j.crm.2017.03.006
[37] Hosmer Jr DW, Lemeshow S, Sturdivant RX. Applied logistic regression. 3rd ed. Hoboken, NJ: Wiley, 2013. DOI: 10.1002/9781118548387
[38] R Core Team. R: A Language and Environment for Statistical Computing, version 4.6.1. Vienna, Austria: R Foundation for Statistical Computing, 2026. Available from: https://www.R-project.org (accessed on 28 September 2026).
[39] Pedregosa F, Varoquaux G, Gramfort A, Michel V, Thirion B, Grisel O, et al. Scikit-learn: Machine learning in Python. Journal of Machine Learning Research, 2011, 12, 2825-2830.
[40] Sole RV, Alonso D, McKane A. Self-organized instability in complex ecosystems. Philosophical Transactions of the Royal Society B, 2002, 357(1421), 667-681. DOI: 10.1098/rstb.2001.0992
[41] Trollope WSW. Controlling bush encroachment with fire in the savanna areas of South Africa. Proceedings of the Annual Congress of the Grassland Society of Southern Africa, 1980, 15, 173-177. DOI: 10.1080/00725560.1980.9648907
[42] Wiens JA. Spatial scaling in ecology. Functional Ecology, 1989, 3(4), 385-397. DOI: 10.2307/2389612
[43] Landis JR, Koch GG. The measurement of observer agreement for categorical data. Biometrics, 1977, 33(1), 159-174. DOI: 10.2307/2529310
[44] Kimutai J, Zachariah M, Nhantumbo B, Nkemelang T, Jain S, Pinto I, et al. El Niño key driver of drought in highly vulnerable Southern African countries. London: Imperial College London, 2024. DOI: 10.25561/110770
[45] Haddad NM, Brudvig LA, Clobert J, Davies KF, Gonzalez A, Holt RD, et al. Habitat fragmentation and its lasting impact on Earth's ecosystems. Science Advances, 2015, 1(2), e1500052. DOI: 10.1126/sciadv.1500052
[46] Chapungu L, Yekeye T. Estimating tree species diversity in small-scale farming areas for effective environmental management: The case of Bindura and Shamva Districts, Zimbabwe. Sacha Journal of Environmental Studies, 2013, 3(1), 23-33.
[47] O'Connor TG, Puttick JR, Hoffman MT. Bush encroachment in southern Africa: Changes and causes. African Journal of Range & Forage Science, 2014, 31(2), 67-88. DOI: 10.2989/10220119.2014.939996
[48] Stevens N, Lehmann CER, Murphy BP, Durigan G. Savanna woody encroachment is widespread across three continents. Global Change Biology, 2017, 23(1), 235-244. DOI: 10.1111/gcb.13409
[49] Venter ZS, Cramer MD, Hawkins HJ. Drivers of woody plant encroachment over Africa. Nature Communications, 2018, 9, 2272. DOI: 10.1038/s41467-018-04616-8
[50] Lord JM, Norton DA. Scale and the spatial concept of fragmentation. Conservation Biology, 1990, 4(2), 197-202. DOI: 10.1111/j.1523-1739.1990.tb00109.x

[51] Hanski I. Metapopulation ecology. Oxford, UK: Oxford University Press, 1999.
[52] Pimm SL. The balance of nature? Chicago, IL: University of Chicago Press, 1991.
[53] Gandiwa P, Matsvayi M, Ngwenya MM, Gandiwa E. Assessment of livestock and human settlement encroachment into northern Gonarezhou National Park, Zimbabwe. Journal of Sustainable Development in Africa, 2011, 13(5), 19-33.
[54] Nyamadzawo G, Gwenzi W, Kanda A, Kundhlande A, Masona C. Understanding the causes, socio-economic and environmental impacts, and management of veld fires in tropical Zimbabwe. Fire Science Reviews, 2013, 2, 2. DOI: 10.1186/2193-0414-2-2
[55] Gandiwa E, Heitkönig IMA, Lokhorst AM, Prins HHT, Leeuwis C. CAMPFIRE and human-wildlife conflicts in local communities bordering northern Gonarezhou National Park, Zimbabwe. Ecology and Society, 2013, 18(4), 7. DOI: 10.5751/ES-05817-180407
[56] Department of National Parks and Wildlife Management. The policy and plan for elephant management in Zimbabwe. Harare: Department of National Parks and Wildlife Management, 1997.